ELSEVIER

www.elsevier.nl/locate/jorganchem

Journal of Organometallic Chemistry 614–615 (2000) 208–214

Journal of Organo metallic Chemistry

Monocarbollide complexes of osmium: X-ray crystal structure of $[Os(CO)_3\{\eta^5\text{-}5\text{-}(NMe_3)\text{-}7\text{-}CB_{10}H_{10}\}]$

Dianne D. Ellis, Andreas Franken, Thomas D. McGrath, F. Gordon A. Stone *

Department of Chemistry and Biochemistry, Baylor University, Waco, TX 76798-7348, USA

Received 18 April 2000

This paper is dedicated to Professor Sheldon Shore and Mildred on the occasion of Sheldon's 70th birthday. Long may the Red Boron fly.

Abstract

In bromobenzene at reflux temperatures the compounds $[Os_3(CO)_{12}]$ and $[N(PPh_3)_2][\textit{nido}\text{-}7\text{-}CB_{10}H_{13}]$ yield a mixture of the anionic tri- and mono-osmium complexes $[Os_3(CO)_8(\eta^5\text{-}7\text{-}CB_{10}H_{11})]^-$ and $[Os(CO)_3(\eta^5\text{-}7\text{-}CB_{10}H_{11})]^-$, respectively, characterized as their $[N(PPh_3)_2]^+$ salts (**2b**, **3c**). Protonation of **2b** with $HBF_4{\cdot}Et_2O$ in thf (tetrahydrofuran) yields the hydrido cluster complex $[Os_3(\mu\text{-}H)(CO)_8(\eta^5\text{-}7\text{-}CB_{10}H_{11})]$ (**4b**), whilst treatment of **2b** in the same solvent with CuCl and PPh_3 in the presence of $TlPF_6$ affords the bimetallic complex $[Os_3(\mu\text{-}H)(CO)_8\{\eta^5\text{-}10\text{-}Cu(PPh_3)\text{-}7\text{-}CB_{10}H_{10}\}]$ (**5b**). In contrast, the compounds $[NHMe_3][\textit{nido}\text{-}7\text{-}CB_{10}H_{13}]$ and $[Os_3(CO)_{12}]$ in refluxing bromobenzene give the novel zwitterionic complex $[Os(CO)_3\{\eta^5\text{-}5\text{-}(NMe_3)\text{-}7\text{-}CB_{10}H_{10}\}]$ (**6**). The structure of **6** was determined by X-ray crystallography, revealing an $Os(CO)_3$ moiety η^5-ligated by the carborane cluster in which, unusually, the NMe_3 ligand is bonded to a boron atom on the upper B_5 belt. © 2000 Elsevier Science B.V. All rights reserved.

Keywords: Osmium; Ruthenium; Carbonyl; Carborane; Crystal structure

---

1. Introduction

Metallacarborane compounds containing *closo*-3,1,2-MC_2B_9 core structures have received extensive study during the past 35 years; however, related species with *closo*-2,1-MCB_{10} frameworks have until recently received only cursory attention [1]. Several aspects of the chemistry of the icosahedral monocarbollide complexes are of interest to us. Studies on metal complexes having the dicarbollide $\eta^5\text{-}7,8\text{-}C_2B_9H_{11}$ ligand have shown that this group frequently adopts a non-spectator role in reactions [2][1]. Though as yet somewhat limited in scope, investigations with $M\{\eta^5\text{-}7\text{-}(NR_3)\text{-}7\text{-}CB_{10}H_{10}\}$ cage systems have shown similar behavior [3,4]. Thus reactions between the monocarbon carboranes *nido*-7-NR_3-7-$CB_{10}H_{12}$ and the metal carbonyls $[M_3(CO)_{12}]$ (M = Ru or Os) afford the neutral charge compensated complexes $[M_3(CO)_8\{\eta^5\text{-}7\text{-}(NR_3)\text{-}7\text{-}CB_{10}H_{10}\}]$ (**1**) in which the cage bridges the metal triangle via two exopolyhedral B–H⇀M bonds.

It was of interest to determine if non-spectator behavior also occurred with those complexes which have an $M(\eta^5\text{-}7\text{-}CB_{10}H_{11})$ framework and several recent studies in our laboratory have revealed that this is so [5–11]. For example, in thf (tetrahydrofuran) at reflux temperatures $[Ru_3(CO)_{12}]$ and $[NHMe_3][\textit{nido}\text{-}7\text{-}CB_{10}H_{13}]$ give $[NHMe_3][Ru_3(CO)_8(\eta^5\text{-}7\text{-}CB_{10}H_{11})]$ (**2a**) [10], a species structurally akin to **1a** as revealed by an X-ray diffraction study. In contrast the reaction between the same carborane salt and $[Fe_3(CO)_{12}]$ yields only a monoiron species $[NHMe_3][Fe(CO)_3(\eta^5\text{-}7\text{-}CB_{10}H_{11})]$ (**3a**) [11]. Herein we develop this chemistry further, reporting some mononuclear and trinuclear osmium monocarbollide complexes.

---

* Corresponding author.

[1] The metallacarboranes discussed in this article have icosahedral frameworks with *closo*-1,2-dicarba-3-metalla-dodecaborane or *closo*-1-carba-2-metalla-dodecaborane structures. However, in the line formulae we represent the cages as *nido*-11-vertex ligands with numbering as for an icosahedron from which the twelfth vertex has been removed. This emphasizes the pentahapto ligating properties of these groups with the cages acting formally as four- and three-electron donors, respectively, to the metal centers in the $M(\eta^5\text{-}7,8\text{-}C_2B_9H_{11})$ and $M(\eta^5\text{-}7\text{-}CB_{10}H_{11})$ complexes.

PII: S0022-328X(00)00578-7

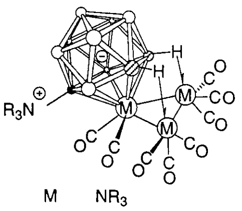

M	NR_3
1a Ru	NMe_3, NH_2Bu^t, NMe_2Bu^t
1b Os	NMe_3

○ BH ▨ B ● C

2. Results and discussion

The salts $[N(PPh_3)_2][Os_3(CO)_8(\eta^5\text{-}7\text{-}CB_{10}H_{11})]$ (**2b**) and $[N(PPh_3)_2][Os(CO)_3(\eta^5\text{-}7\text{-}CB_{10}H_{11})]$ (**3c**) are formed in roughly equal proportions when $[Os_3(CO)_{12}]$ and $[N(PPh_3)_2]$[*nido*-7-$CB_{10}H_{13}$] are refluxed in bromobenzene for 7 h (Scheme 1). Formally the two μ-H atoms of [*nido*-7-$CB_{10}H_{13}]^-$ are reduced to dihydrogen with a corresponding $2e^-$ oxidation of the osmium. More prolonged reaction times do not significantly improve formation of **3c**. Indeed the somewhat forcing conditions employed instead increased decomposition. Data characterizing **2b** and **3c** are summarized in Tables 1–3.

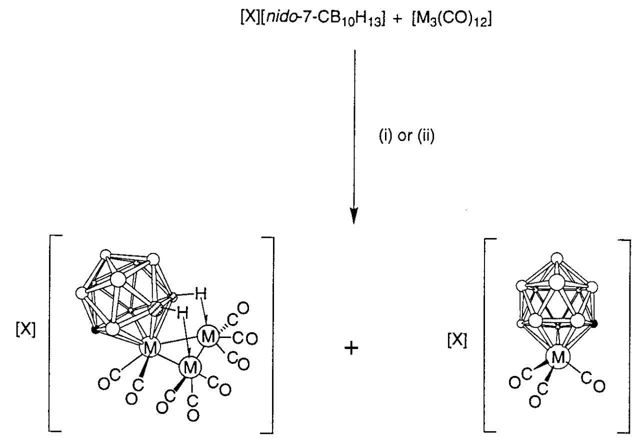

X	M
2a $NHMe_3$	Ru
2b $N(PPh_3)_2$	Os

X	M
3a $NHMe_3$	Fe
3b $NHMe_3$	Ru
3c $N(PPh_3)_2$	Os

○ BH ▨ B ● CH

Scheme 1. (i) M = Fe or Ru, in thf, reflux or (ii) M = Os, in C_6H_5Br, reflux.

As expected the spectroscopic properties of **2b** are very similar to those of its ruthenium analog **2a** [10]. Both

Table 1
Analytical and physical data

Compound [a]	Yield (%)	$\nu_{max}(CO)$ [b] (cm^{-1})	Anal. (%) [c]	
			C	H
$[N(PPh_3)_2][Os_3(CO)_8(\eta^5\text{-}7\text{-}CB_{10}H_{11})]$ (**2b**)	35	2047 s, 2035 s, 2017 s, 2000 s, 1982 m	35.7 (36.9)	2.5 (2.8)
$[N(PPh_3)_2][Os(CO)_3(\eta^5\text{-}7\text{-}CB_{10}H_{11})]$ (**3c**)	41	2076 s, 1993 s	50.3 (50.9)	4.4 (4.4)
$[Os_3(\mu\text{-}H)(CO)_8(\eta^5\text{-}7\text{-}CB_{10}H_{11})]$ (**4b**)	40	2130 s, 2106 s, 2047 s, 2017 m, 1970 w	12.2 (11.7)	1.3 (1.3)
$[Os_3(\mu\text{-}H)(CO)_8\{\eta^5\text{-}10\text{-}Cu(PPh_3)\text{-}7\text{-}CB_{10}H_{10}\}]$ (**5b**)	50	2076 m, 2035 s, 2017 s, 1999 s, 1970 m	25.8 (25.9)	1.6 (2.1)
$[Os(CO)_3\{\eta^5\text{-}5\text{-}(NMe_3)\text{-}7\text{-}CB_{10}H_{10}\}]$ (**6**)	38	2088 s, 2017 s	18.4 (18.1)	4.2 (4.1)

[a] All compounds are yellow in colour, except **3b**, which is red.
[b] Measured in CH_2Cl_2; medium-intensity bands observed at ca. 2550 cm^{-1} in the spectra of all compounds are due to B–H adsorptions.
[c] Calculated values are given in parentheses.

Table 2
^1H and ^{13}C-NMR data [a]

Compound	^1H (δ) [b]	^{13}C (δ) [c]
2b	−13.10 [br q, 2H, B–H⇀Os, J(BH) = 61], 1.55 (s, 1H, cage CH), 7.49 (m, 30 H, Ph)	184.1, 183.1, 179.3, 176.6, 172.7 (CO), 134.0–126.7 (Ph), 26.8 (cage CH)
3c	1.57 (s, 1H, cage CH), 7.49 (m, 30H, Ph)	179.1 (CO), 134.0–126.7 (Ph), 36.6 (cage CH)
4b	−18.65 (s, 1H, μ-H), −13.50 [br q, 2H, B–H⇀Os, J(BH) = 45], 2.81 (s, 1H, cage CH)	180.1, 171.5, 165.0, 163.0 (CO), 31.3 (cage CH)
5b	−19.89 (s, 1H, μ-H), −13.50 [br q, 2H, B–H⇀Os, J(BH) = 42], 2.91 (s, 1H, cage CH), 7.50 (m, 15H, Ph)	182.5, 180.7, 175.3, 173.4, 172.3, 170.9, 165.8, 165.0 (CO), 134.0–129.4 (Ph), 49.2 (cage CH)
6	2.11 (s, 1H, cage CH), 2.81 (s, 9H, Me)	176.6 (CO), 56.1 (Me), 32.9 (cage CH)

[a] Chemical shifts (δ) in ppm, coupling constants (J) in Hertz, measurements at ambient temperature in CD_2Cl_2.
[b] Resonances for terminal BH protons occur as broad unresolved signals in the range δ ca. −1 to 3.
[c] ^1H-decoupled chemical shifts are positive to high frequency of $SiMe_4$.

Table 3
^{11}B and ^{31}P-NMR data [a]

Compound	^{11}B (δ) [b]
2b	12.4 [2B, B–H$\rightharpoonup$Os, J(HB) = 61], −1.6 (1B), −7.8 (1B), −12.4 (4B), −17.4 (2B)
3b	8.8 (1B), −5.1 (2B), −7.7 (3B), −14.3 (2B), −17.6 (2B)
3c	7.0 (1B), −8.2 (1B), −10.3 (2B), −12.4 (2B), −16.0 (2B), −19.2 (2B)
4b	13.1 [2B, B–H$\rightharpoonup$Os, J(HB) = 45], 1.6 (1B), −10.52 (3B), −11.0 (2B), −15.4 (2B)
5b [c]	29.1 (1B, B–Cu), 16.2 [1B, B–H$\rightharpoonup$Os, J(HB) = 42], 1.1 (1B), −8.5 (1B), −13.1 (4B), −14.3 (2B)
6	5.9 (s, 1B, B–NMe$_3$), 3.4 (1B), −12.9 (2B), −15.2 (2B), −18.0 (2B), −19.8 (2B)

[a] Measurements at ambient temperature in CD_2Cl_2.

[b] ^{1}H-decoupled chemical shifts (δ) are positive to high frequency of $BF_3{\cdot}Et_2O$ (external). Signals ascribed to more than one boron nucleus may result from overlapping peaks and do not necessarily indicate symmetry equivalence. The ^{1}H–^{11}B coupling constants [J(BH)] were measured from fully coupled ^{11}B spectra.

[c] ^{31}P{^{1}H}-NMR δ 6.9 (br), chemical shift is positive to high frequency of 85% H_3PO_4 (external).

molecules display five CO stretching bands in their IR spectra. In their ^{1}H-NMR spectra broad quartets are seen corresponding in intensity to two protons for the B–H$\rightharpoonup$M (Ru, Os) bonds [**2a** δ −10.63, J(BH) = 68 Hz; **2b** δ −13.10, J(BH) = 61 Hz]. The ^{13}C{^{1}H}-NMR spectrum of **2b** revealed a resonance for the cage CH group at δ 26.8 which compares with that seen in the spectrum of **2a** at δ 33.9. The ^{11}B{^{1}H}-NMR data for **2b** and **2a** show 2:1:1:4:2 and 2:1:1:2:2:2 patterns, respectively, in accordance with C_s molecular symmetry in both anions. The mirror plane encompasses the cage Os and C atoms and the midpoint of the $(OC)_3Os$–$Os(CO)_3$ bond and allows assignment of **2b** as the β,β-isomer; both B–H$\rightharpoonup$Os bonds involve boron atoms which lie in positions β to the cage carbon vertex in the pentahapto $\overline{\text{CB}\textit{BB}\text{B}}$ ring ligating the third Os atom. In the ^{11}B{^{1}H}-NMR spectrum of **2b** the resonance for the B–H$\rightharpoonup$Os nucleus is assigned to a peak at δ 12.4 which becomes a doublet [J(HB) = 61 Hz] in a fully coupled ^{11}B spectrum [12]. The corresponding signal in the ^{11}B{^{1}H}-NMR spectrum of **2a** is at δ 18.8, also appearing as a doublet in the ^{11}B spectrum [J(HB) = 67 Hz] [10].

Following our earlier work [10] further studies on the reaction between [NHMe$_3$][*nido*-7-$CB_{10}H_{13}$] and [$Ru_3(CO)_{12}$] confirmed the synthesis of **2a** in very high yield (ca. > 90%) but also we have now found there is evidence for formation in very low yields of the monoruthenium complex [NHMe$_3$][Ru(CO)$_3$(η^5-7-$CB_{10}H_{11}$)] (**3b**). Unfortunately this species could not be separated from its precursor [NHMe$_3$][*nido*-7-$CB_{10}H_{13}$] by column chromatography. However, IR bands for CO groups were measured at 2079 and 2014 cm^{-1} which may be compared with those seen in the spectra of **3c** at 2076 and 1993 cm^{-1} (Table 1), and **3a** at 2065 and 1999 cm^{-1} [11]. Moreover, examination of the ^{1}H and ^{13}C{^{1}H}-NMR spectra of solutions enriched in **3b** revealed signals at δ 2.21 (^{1}H) and 34.3 (^{13}C{^{1}H}) which may be assigned to a ligated cage CH group. ^{11}B-NMR parameters for **3b** are given in Table 3.

Protonation of **2b** with $HBF_4{\cdot}Et_2O$ affords the neutral complex [Os_3(μ-H)(CO)$_8$(η^5-7-$CB_{10}H_{11}$)] (**4b**) (Scheme 2). Comparison of the NMR data for the latter (Tables 2 and 3) with those of **4a** [10] establishes the close similarity between these compounds. In the ^{1}H-NMR spectrum of **4b** a resonance for the bridging Os(μ-H)Os ligand is seen at δ −18.65. This may be compared with the corresponding resonance for **4a** at δ −19.03. A quartet with broad peaks at δ −13.50 [J(BH) = 45 Hz], corresponding in intensity to two protons, may be assigned to the two B–H$\rightharpoonup$Os linkages, and a further signal at δ 2.81 of unit relative intensity is in the region characteristic of a cage CH. In the ^{11}B{^{1}H}-NMR spectrum a resonance at δ 13.1, integrating to 2 B and which became a doublet [J(HB) = 45 Hz] in a fully coupled ^{11}B spectrum, is very similar to the corresponding data for **2b**. Like the parent anion, the presence of a plane of mirror symmetry in **4b** through the cage Os and C atoms and the midpoint of the $(OC)_3Os$–$Os(CO)_3$ bond is reflected in the observed ^{1}H and ^{11}B{^{1}H}-NMR data, the latter showing a 2:1:3:2:2 set of resonances.

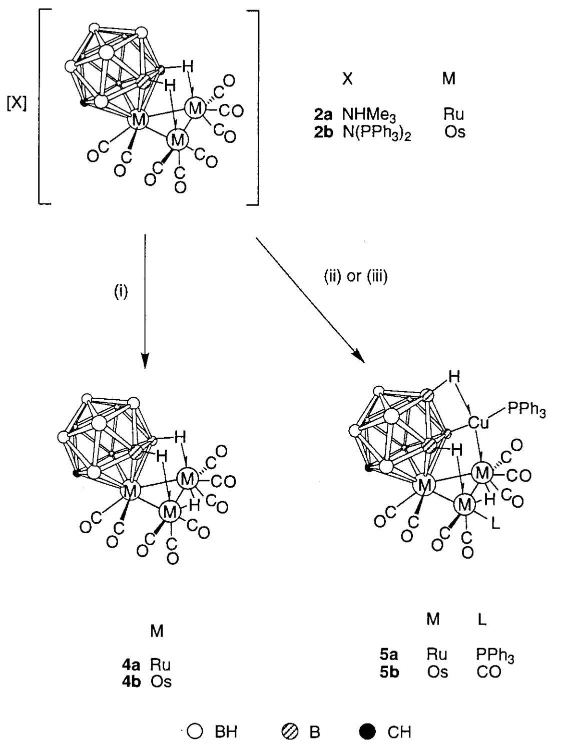

Scheme 2. (i) $HBF_4{\cdot}Et_2O$ in thf. (ii) M = Ru, thf solvent, [CuCl(PPh$_3$)$_3$], TlPF$_6$. (iii) M = Os, thf solvent, CuCl, PPh$_3$, TlPF$_6$.

The $[Cu(PPh_3)]^+$ group, isolobal with the proton, also reacts with **2b**, affording a bimetallic cluster. Thus, when **2b** was treated with CuCl and PPh_3 in thf, with $TlPF_6$ added to remove chloride as insoluble TlCl, the reaction yielded the cluster compound $[Os_3(\mu\text{-}H)(CO)_8\{\eta^5\text{-}10\text{-}Cu(PPh_3)\text{-}7\text{-}CB_{10}H_{10}\}]$ (**5b**). Compound **5b** differs from the related triruthenium species **5a** in that it bears no metal-bound phosphine group. The presence of this latter feature in **5a** [10] arose from use of $[CuCl(PPh_3)_3]$ as a source of the copper fragment, and excess PPh_3 released by this reagent provided the additional phosphine for substitution on the ruthenium, whereas in the synthesis of **5b** no such excess PPh_3 was available to the cluster. Despite this difference in constitution, both **5a** and **5b** show otherwise very similar spectroscopic features and **5b** is reasonably assigned the structure shown (Scheme 2) by analogy with **5a** for which a single-crystal X-ray diffraction study was made [10]. The NMR data for **5b** are given in Tables 2 and 3. In the ^1H-NMR spectrum the $B\text{–}H\rightharpoonup Os$ group displays a diagnostic quartet at δ -13.50 [$J(BH) = 42$ Hz] and a singlet resonance for the $Os(\mu\text{-}H)Os$ moiety is seen at δ -19.89. As was noted previously for **5a** [10], no signal attributable to the proton involved in the $B\text{–}H\rightharpoonup Cu$ linkage was found, presumably a consequence of dynamic behavior. In the $^{11}B\{^1H\}$-NMR spectrum of **5b** a signal at δ 29.1, which remains a singlet in the fully coupled ^{11}B spectrum, may be assigned to the B(10)–Cu group, while the resonance at δ 16.2 can be attributed to the boron atom of the $B\text{–}H\rightharpoonup Os$ group as it becomes a doublet with $J(HB) = 42$ Hz in the fully coupled ^{11}B spectrum. The $^{31}P\{^1H\}$-NMR spectrum shows a signal at δ 6.9, which may be assigned to the $Cu(PPh_3)$ group and which is broadened by the adjacent quadrupolar boron and copper nuclei.

The neutral zwitterionic species $[Os(CO)_3\{\eta^5\text{-}5\text{-}(NMe_3)\text{-}7\text{-}CB_{10}H_{10}\}]$ (**6**) (Scheme 3) is formed when $[Os_3(CO)_{12}]$ and the $[NHMe_3]^+$ salt of $[nido\text{-}7\text{-}CB_{10}H_{13}]^-$ are heated in bromobenzene to reflux temperatures. Compound **6** was unambiguously identified by an X-ray diffraction study, which revealed the molecular structure shown in Fig. 1. Selected internuclear distances and angles are listed in Table 4. Among the monocarbon metallacarboranes, **6** is unique in having the two-electron donor NMe_3 group σ-bonded to a boron vertex in the upper B_5 belt. Thus, although overall a neutral species, compound **6** is zwitterionic with a positively charged nitrogen atom attached to the monoanionic cluster. The osmium atom is essentially symmetrically bound to all five atoms of the ligating $\overline{CBBBB}$ carborane face at distances comparable with those in **1b** [4]. Of the three exopolyhedral carbonyl ligands the one which lies approximately *trans* to the cage-carbon atom appears slightly more closely bound. At 1.57(2) Å, the B–N distance is unremarkable. Spectroscopic data characterizing **6** are given in Tables 1–3. The ^{11}B-NMR spectrum was informative showing a 1:1:2:2:2:2 intensity pattern, thus indicating the presence of a mirror plane (encompassing the cage Os and C atoms and the B(5)–N group), and is consistent with the approximate molecular mirror symmetry determined in the solid state structure. In the fully coupled ^{11}B-NMR spectrum a singlet resonance at δ 5.9 may be assigned to the $B(5)\text{–}NMe_3$ group. The site of B-substi-

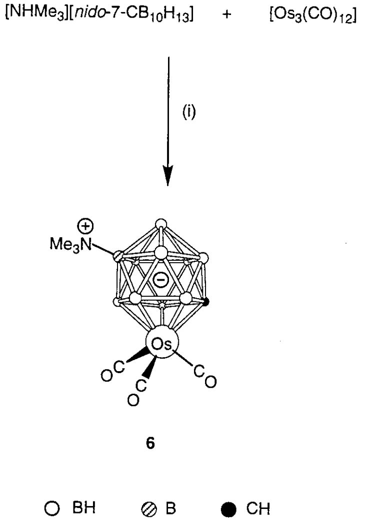

Scheme 3. (i) C_6H_5Br reflux.

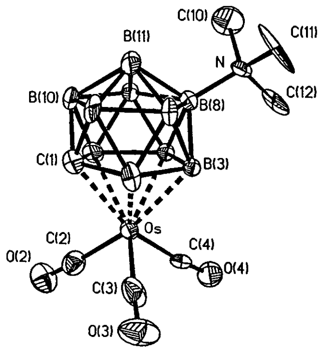

Fig. 1. Structure of $[Os(CO)_3\{\eta^5\text{-}5\text{-}(NMe_3)\text{-}7\text{-}CB_{10}H_{10}\}]$ (**6**) showing the crystallographic labeling scheme. Hydrogen atoms are omitted for clarity and thermal ellipsoids are shown at the 40% probability level.

Table 4
Selected interatomic distances (Å) and angles (°) for compound **6**

Os–C(1)	2.273(14)	Os–C(2)	1.93(2)
Os–B(2)	2.26(2)	Os–C(3)	1.91(2)
Os–B(3)	2.29(2)	Os–C(4)	1.88(2)
Os–B(4)	2.29(2)	C(2)–O(2)	1.13(2)
Os–B(5)	2.25(2)	C(3)–O(3)	1.14(2)
B(8)–N	1.57(2)	C(4)–O(4)	1.15(2)
C(3)–Os–C(2)	93.2(6)	O(2)–C(2)–Os	174(2)
C(4)–Os–C(3)	90.7(7)	O(3)–C(3)–Os	177(2)
C(4)–Os–C(2)	91.2(6)	O(4)–C(4)–Os	172.2(14)

tution in **6** is of interest, because in such *closo*-2,1-MCB_{10} clusters, we have previously observed boron-atom substitution only on the $\overline{\text{CBBBB}}$ ring ligating the metal center [9,11]. It may be that substitution at the boron atom antipodal to the cage carbon atom (as observed here) is at a thermodynamically preferred site as a result of the somewhat elevated reaction temperatures employed in the synthesis of this compound. The pathway by which **6** is formed is unknown at the present time and in the absence of other products one may only speculate as to whether ligand attachment occurs before or after metal ligation and as to whether any skeletal rearrangement occurs by which a ligand bound at B(9) (for example) might migrate to B(5). The source of the NMe_3 group is clearly the cation of the reagent $[NHMe_3]$[*nido*-7-$CB_{10}H_{13}$].

3. Conclusions

The work described herein together with that reported earlier [10,11] reveals that the nature of the products formed in reactions between the metal carbonyls $[M_3(CO)_{12}]$ (M = Fe, Ru, Os) and the carborane [*nido*-7-$CB_{10}H_{13}]^-$ varies with the metal and with the cation with which the anion is associated. The iron carbonyl with $[NHMe_3]$[*nido*-7-$CB_{10}H_{13}$] in refluxing thf forms the monoiron complex $[NHMe_3][Fe(CO)_3(\eta^5\text{-}7\text{-}CB_{10}H_{11})]$. Ruthenium carbonyl under the same conditions affords predominantly the trimetal species $[NHMe_3][Ru_3(CO)_8(\eta^5\text{-}7\text{-}CB_{10}H_{11})]$. Osmium carbonyl requires higher temperatures (refluxing bromobenzene) for reaction and with $[NHMe_3]$[*nido*-7-$CB_{10}H_{13}$] gives unexpectedly the charge-compensated species $[Os(CO)_3\{\eta^5\text{-}5\text{-}(NMe_3)\text{-}7\text{-}CB_{10}H_{10}\}]$ (**6**). If $[N(PPh_3)_2]$[*nido*-7-$CB_{10}H_{13}$] is used as the reagent, essentially equal amounts of monoosmium $[N(PPh_3)_2][Os(CO)_3(\eta^5\text{-}7\text{-}CB_{10}H_{11})]$ (**3c**) and triosmium $[N(PPh_3)_2][Os_3(CO)_8(\eta^5\text{-}7\text{-}CB_{10}H_{11})]$ (**2b**) are produced. Clearly the new osmacarboranes merit further study as precursors to new complexes, as indicated by the protonation of **2b** and its reaction with $[Cu(PPh_3)]^+$.

4. Experimental

4.1. General considerations

Solvents were distilled from appropriate drying agents under nitrogen prior to use. Petroleum ether refers to that fraction of boiling point 40–60°C. All reactions were carried out under an atmosphere of dry nitrogen using Schlenk line techniques. Chromatography columns (ca. 15 cm in length and ca. 2 cm in diameter) were packed with silica gel (Aldrich, 70-230 mesh). TLC was performed on preparative Uniplates (silica gel G, Analtech). NMR spectra were recorded at the following frequencies: ^1H 360.1, ^{13}C 90.6, ^{31}P 145.7, and ^{11}B 115.5 MHz. The salts $[NHMe_3]$[*nido*-7-$CB_{10}H_{13}$] and $[N(PPh_3)_2]$[*nido*-7-$CB_{10}H_{13}$] were synthesized from *nido*-7-NMe_3-7-$CB_{10}H_{12}$ according to the method of Knoth and coworkers [13].

4.2. Synthesis of $[N(PPh_3)_2][Os_3(CO)_8(\eta^5\text{-}7\text{-}CB_{10}H_{11})]$ and $[N(PPh_3)_2][Os(CO)_3(\eta^5\text{-}7\text{-}CB_{10}H_{11})]$

The compounds $[Os_3(CO)_{12}]$ (0.45 g, 0.50 mmol) and $[N(PPh_3)_2]$[*nido*-7-$CB_{10}H_{13}$] (0.10 g, 0.50 mmol) were heated at reflux in bromobenzene (10 ml) for 7 h. The mixture was then cooled to room temperature, solvent was removed in vacuo, and the residue was treated with CH_2Cl_2 (15 ml). After filtration, ca. 2 g of silica gel was added to the filtrate. Solvent was removed in vacuo affording a yellow–brown powder which was transferred to the top of a chromatography column. Elution with CH_2Cl_2–petroleum ether (3:1) gave first a yellow fraction. Removal of solvent in vacuo yielded $[N(PPh_3)_2][Os_3(CO)_8(\eta^5\text{-}7\text{-}CB_{10}H_{11})]$ (**2b**) (0.26 g) as yellow microcrystals. Further elution with pure CH_2Cl_2 gave a second yellow fraction which after removal of solvent in vacuo yielded $[N(PPh_3)_2][Os(CO)_3(\eta^5\text{-}7\text{-}CB_{10}H_{11})]$ (**3c**) (0.19 g) as a yellow powder. The products **2b** and **3c** so obtained were sufficiently pure for further reaction; analytically pure samples could be obtained by further column chromatography, followed by recrystallization from CH_2Cl_2–petroleum ether.

4.3. Protonation of $[N(PPh_3)_2][Os_3(CO)_8(\eta^5\text{-}7\text{-}CB_{10}H_{11})]$

Compound **2b** (0.30 g, 0.20 mmol) was dissolved in thf (10 ml), $HBF_4 \cdot Et_2O$ (0.10 ml) was added and the solution was stirred for 1 h. Solvent was removed in vacuo, and the residue was treated with CH_2Cl_2 (15 ml). After filtration, ca. 2 g of silica gel was added to the filtrate. Solvent was removed in vacuo affording a yellow powder which was transferred to the top of a chromatography column. Elution with CH_2Cl_2–petroleum ether (3:2) gave a yellow fraction. Removal of solvent in vacuo followed by crystallization from CH_2Cl_2–petroleum ether yielded yellow microcrystals of $[Os_3(\mu\text{-}H)(CO)_8(\eta^5\text{-}7\text{-}CB_{10}H_{11})]$ (**4b**) (0.076 g).

4.4. Synthesis of the triosmium–copper complex

Compound **2b** (0.37 g, 0.25 mmol) was dissolved in thf (10 ml) and CuCl (0.03 g, 0.25 mmol), PPh_3 (0.07g, 0.25 mmol), and $TlPF_6$ (0.09 g, 0.25 mmol) were added. After stirring the mixture at room temperature for ca. 12 h, solvent was removed in vacuo and the yellow residue was extracted with CH_2Cl_2 (15 ml). After filtration, ca. 2 g of silica gel was added to the filtrate,

Table 5
Crystallographic data for **6**

Formula	$C_7H_{19}B_{10}NO_3Os$	$F(000)$	1744
M_r	463.53	θ range (°)	2.36–22.50
Crystal color, habit	Yellow–orange block	Index ranges	$-14 \leq h \leq 0$, $0 \leq k \leq 14$, $-18 \leq l \leq 0$
Crystal size (mm)	0.49 × 0.46 × 0.45	Reflections collected	2115
Crystal system	Orthorhombic	Independent reflections	2115 [$R_{int} = 0.0000$]
Space group	*Pbca*	Observed reflections [$I > 2\sigma(I)$]	1389
Unit cell parameters		T_{max}, T_{min}	0.8398, 0.6886
a (Å)	13.646(2)	Refinement method [a]	Full-matrix least-squares on F^2
b (Å)	13.707(3)	Final R indices [$I > 2\sigma(I)$]	$R_1 = 0.0468$, $wR_2 = 0.0841$
c (Å)	17.267(5)	R indices (all data)	$R_1 = 0.0883$, $wR_2 = 0.0969$
V (Å^3)	3229.8(12)	Goodness-of-fit on F^2	1.114
Z	8	Extinction coefficient	0.00031(4)
D_{calc} (g cm^{-3})	1.907	Maximum, minimum residual electron density (e Å^{-3})	0.881, −0.972
μ (mm^{-1})	7.895		

[a] Structure was refined on F_o^2 using all data with weighting scheme $w^{-1} = [\sigma^2(F_o^2) + (0.0290P)^2]$ where $P = (F_o^2 + 2F_c^2)/3$.

solvent was removed in vacuo and the yellow powder obtained was transferred to the top of a chromatography column. Elution with CH_2Cl_2–petroleum ether (3:2) gave a yellow fraction. Removal of solvent in vacuo followed by crystallization from CH_2Cl_2–petroleum ether yielded yellow microcrystals of $[Os_3(\mu\text{-}H)(CO)_8\{\eta^5\text{-}10\text{-}Cu(PPh_3)\text{-}7\text{-}CB_{10}H_{10}\}]$ (**5b**) (0.16 g).

4.5. Synthesis of $[Os(CO)_3\{\eta^5\text{-}5\text{-}(NMe_3)\text{-}7\text{-}CB_{10}H_{10}\}]$

The compounds $[Os_3(CO)_{12}]$ (0.45 g, 0.50 mmol) and $[NHMe_3][$*nido*$\text{-}7\text{-}CB_{10}H_{13}]$ (0.10 g, 0.52 mmol) were heated at reflux in bromobenzene (10 ml) for 12 h. The mixture was then cooled to room temperature, solvent was removed in vacuo, and the residue was treated with CH_2Cl_2 (15 ml). After filtration, ca. 2 g of silica gel was added to the filtrate. Solvent was removed in vacuo affording a yellow–brown powder which was transferred to the top of a chromatography column. Elution with CH_2Cl_2–petroleum ether (3:2) gave a yellow fraction. Removal of solvent in vacuo followed by crystallization from CH_2Cl_2–petroleum ether yielded yellow microcrystals of $[Os(CO)_3\{\eta^5\text{-}5\text{-}(NMe_3)\text{-}7\text{-}CB_{10}H_{10}\}]$ (**6**) (0.09 g).

4.6. X-ray structural analysis

Suitable crystals of **6** were obtained by slow diffusion of a CH_2Cl_2 solution and pentane at ambient temperature. Crystal data and details of structure solution and refinement are summarized in Table 5. Diffracted intensities were collected at 293(2) K on an Enraf–Nonius CAD-4 diffractometer operating in the ω–2θ scan mode, using graphite-monochromated Mo–K_α X-radiation ($\lambda = 0.71073$ Å). Final unit cell dimensions were determined from the setting angles of 25 accurately centered reflections. Crystal stability during data collection was monitored by measuring the intensities of three standard reflections every 2 h. Data were collected at a constant scan speed of 5.17° min^{-1} in ω, with a scan range of $1.15° + 0.34 \tan\theta$. The data were corrected for Lorentz, polarization and X-ray absorption effects, the latter by a semi-empirical method based on azimuthal ψ scans.

The structure was solved by direct methods and developed by successive Fourier difference syntheses, using SHELXTL-PC version 4.1 [14]. Refinement was by full-matrix least-squares on F^2 using SHELXL-93, with anisotropic thermal parameters for all non-hydrogen atoms, except B(3) and B(4) which were refined with isotropic thermal parameters. All hydrogen atoms were included in calculated positions and allowed to ride on their parent boron or carbon atom with calculated isotropic thermal parameters equal to 1.2 (B–H or cage CH) or 1.5 (Me) times U_{iso} of the parent atom. Residual electron density was found in the difference Fourier syntheses near the Os atom.

5. Supplementary material

Atomic coordinates, a complete listing of bond lengths and angles, and the thermal parameters for **6** have been deposited at the Cambridge Crystallographic Data Centre, CCDC no. 143206. Copies of this information may be obtained free of charge from The Director, CCDC, 12 Union Street, Cambridge CB2 1EZ, UK (Fax: +44-1223-336033; e-mail: deposit@ccdc.cam.ac.uk or www: http://www.ccdc.cam.ac.uk).

Acknowledgements

We thank the Robert A. Welch Foundation for support (Grant AA-1201).

References

[1] For leading refs. see: R.N. Grimes, in: E.W. Abel, F.G.A. Stone, G. Wilkinson (Eds.), Comprehensive Organometallic Chemistry II, vol. 1 (C.E. Housecroft (Ed.)), Pergamon, Oxford, 1995, Chapter 9. R.N. Grimes, in: G. Wilkinson, E.W. Abel, F.G.A. Stone (Eds.), Comprehensive Organometallic Chemistry I, Pergamon, Oxford, 1982, Chapter 5.5.

[2] P.A. Jelliss, F.G.A. Stone, J. Organomet. Chem. 500 (1995) 307.

[3] V.N. Lebedev, D.F. Mullica, E.L. Sappenfield, F.G.A. Stone, Organometallics 15 (1996) 1669.

[4] V.N. Lebedev, D.F. Mullica, E.L. Sappenfield, F.G.A. Stone, J. Organomet. Chem. 536-537 (1997) 537.

[5] S.A. Batten, J.C. Jeffery, P.L. Jones, D.F. Mullica, M.D. Rudd, E.L. Sappenfield, F.G.A. Stone, A. Wolf, Inorg. Chem. 36 (1997) 2570.

[6] I. Blandford, J.C. Jeffery, P.A. Jelliss, F.G.A. Stone, Organometallics 17 (1998) 1402.

[7] J.C. Jeffery, P.A. Jelliss, L.H. Rees, F.G.A. Stone, Organometallics 17 (1998) 2258.

[8] I. Blandford, J.C. Jeffery, H. Redfearn, L.H. Rees, M.D. Rudd, F.G.A. Stone, J. Chem. Soc. Dalton Trans. (1998) 1669.

[9] S.A. Batten, J.C. Jeffery, L.H. Rees, M.D. Rudd, F.G.A. Stone, J. Chem. Soc. Dalton Trans. (1998) 2839.

[10] D.D. Ellis, A. Franken, F.G.A. Stone, Organometallics 18 (1999) 2362.

[11] D.D. Ellis, A. Franken, P.A. Jelliss, F.G.A. Stone, P-Y. Yu, Organometallics 19 (2000) 1993.

[12] S.A. Brew, F.G.A. Stone, Adv. Organomet. Chem. 35 (1993) 135.

[13] W.H. Knoth, J.L. Little, J.R. Lawrence, F.R. Scholer, L.J. Todd, Inorg. Synth. 11 (1968) 33.

[14] SHELXTL-PC, Siemens Analytical X-ray Instruments, Madison, WI, 1989.